

Cite this: *RSC Adv.*, 2015, 5, 5244

A novel sensitive fluorescent turn-on probe for rapid detection of Al³⁺ and bioimaging†

Shuai Xia,^a Si-Yu Xiao,^a Qing-Qing Hong,^a Jing-Rong Zou,^a Sen Yang,^a Mu-Xue Zhang^b and Hua Zuo^{*a}

Taking advantage of the condensation reaction of 1-(2-hydroxyphenyl)ethanone and a rhodamine-B derived hydrazide, the first simply-structured rhodamine based probe L for the detection of Al³⁺ with high efficiency was designed and synthesized which could be applied in water solutions. Spectroscopy showed that the probe responded quickly and selectively to Al³⁺ over other metal ions with remarkable fluorescence enhancement (43-fold) after 10 equiv. of Al³⁺ were added. Sensing of Al³⁺ was proved to be effective over a wide pH range from 4.9 to 8.5 and the limit of the detection was calculated as 1.63×10^{-7} M by the fluorescence titration experiment. Besides, the probe L is characterized with good stability and performed perfectly in a reversibility test with EDTA. Furthermore, live-cell imaging of HeLa cells revealed the cell permeability of the probe, showing no toxicity in cultured cells by MTT method, which indicated that L could be applied in living organisms.

Received 9th November 2014
Accepted 11th December 2014

DOI: 10.1039/c4ra14177f

www.rsc.org/advances

Introduction

The fluorescence chemosensing technique, characterized by high sensitivity and selectivity, short response time, operational simplicity and a wide range of applicability, stands out among the many sensing techniques suitable for recognizing metal ions and has featured extensively in analytical chemistry.^{1–5} Besides the detection of metal ions, this technique has been applied in sensing pesticides, dynamite, biomolecules and even cancer cells.^{6–11} Furthermore, compared with traditional sensing techniques such as atomic absorption spectroscopy, inductively coupled plasma-mass spectroscopy and inductively coupled plasma-atomic emission spectroscopy, fluorescence chemosensors turn out to be more cost-efficient.^{12,13}

Aluminum, the most abundant metal and the third most prevalent element in the biosphere, are widely dispersed and applied in modern world: in natural water body, food additives, medicines and as certain kinds of light alloy. However, the intensified environmental acidification enables to dissolve more Al minerals at lower pH, resulting in more amount of the Al³⁺ available¹⁴ which is fatal to the living plants.¹⁵ On the other hand, although it is proverbial that aluminum is a non-essential element for living system, the size and the charge of Al³⁺ make it a competitive inhibitor of several essential elements of similar properties such as Mg²⁺, Ca²⁺ and Fe³⁺.¹⁶ Besides, the

disequilibrium of aluminium homeostasis is implicated in various kinds of diseases, such as Al-related bone disease (ARBD),¹⁷ microcytic hypochromic anemia¹⁸ and especially the noted Parkinson's disease.¹⁹ According to a WHO report, the average daily human intake of aluminium is approximate 3–10 mg and the tolerable weekly aluminium intake in the human body is estimated to be 7 mg kg^{−1} body weight.²⁰

However, due to the poor coordination ability of Al³⁺ compared to transition metals and the lack of spectroscopic properties, the detection of Al³⁺ has always been problematic.²¹ To our best knowledge very few Al³⁺ selective fluorescence probes have been reported, majority of which possess the drawbacks: the water solubility of Al³⁺ probe derived from 8-hydroxyquinoline is very poor,²² the salicylaldehyde Schiff based Al³⁺ probe suffers from low stability²³ and the fluorescence sensor using a molecularly imprinted recognition receptor for the detection of Al³⁺ is strongly interfered by Cu²⁺.²⁴ Furthermore, because of the toxicity to the living cells, the practical use of some Al³⁺ chemosensors is severely hampered.^{25,26}

For another side, the introduction of rhodamine skeleton to the molecule could produce the emission of long-wavelength fluorophore, which is preferred to be considered as reporting group for analyte so as to avoid the inference of background fluorescence (<400 nm).^{27,28} Besides, featured as high quantum yields, large extinction coefficient, great photostability, good water solubility and low toxicity, rhodamine framework is an ideal mode for constructing turn-on fluorescence chemosensors.^{29–31} A large number of rhodamine-based derivatives have been reported to perform as probes to detect metal ions for various intentions.^{32–41} However, no rhodamine-based Al³⁺ selective fluorescence probes have been reported by now

^aCollege of Pharmaceutical Sciences, Southwest University, Chongqing, 400716, China.
E-mail: zuohua@swu.edu.cn; Fax: +86 23 6825 1225; Tel: +86 23 6825 1225

^bCollege of Resources and Environments, Southwest University, Chongqing, 400716, China

† Electronic supplementary information (ESI) available. See DOI: 10.1039/c4ra14177f

because the poor coordination ability of Al^{3+} makes the probes to suffer from interference by other metals. Besides, 1-(2-hydroxyphenyl)ethanone, with one hydroxyl which may enhance the solubility and coordination ability of probe, could be attached to the rhodamine-B frame for that the acetyl is possible to be condensed with the rhodamine-B derivatives. Therefore, we believe that it is feasible to construct novel molecules which owns a perfect coordination pocket by combining the rhodamine-B skeleton with 1-(2-hydroxyphenyl)ethanone.

Herein, through introducing 1-(2-hydroxyphenyl)ethanone to the rhodamine-B derived skeleton, we designed and synthesized the first novel rhodamine-based probe by two simple steps for the detection of Al^{3+} with high selectivity, good stability, perfect reversibility and no toxicity. With the limit of detection of $1.63 \times 10^{-7} \text{ M}$, the probe could be successfully utilized in HeLa cells for sensing trace amount of Al^{3+} because of its excellent cell permeability and no toxicity.

Experimental section

Materials and methods

Deionized water was used throughout the experiment. All the reagents were purchased from commercial suppliers and utilized without further purification. All samples were prepared at room temperature, shaken for 10 s before UV-vis and fluorescence detection. The solutions of metal ions were prepared from $\text{Al}(\text{NO}_3)_3 \cdot 9\text{H}_2\text{O}$, $\text{Ba}(\text{NO}_3)_2$, $\text{Ca}(\text{NO}_3)_2 \cdot 4\text{H}_2\text{O}$, $\text{Co}(\text{NO}_3)_2 \cdot 6\text{H}_2\text{O}$, CsNO_3 , $\text{Cu}(\text{NO}_3)_2 \cdot 3\text{H}_2\text{O}$, $\text{Fe}(\text{NO}_3)_3 \cdot 9\text{H}_2\text{O}$, $\text{Hg}(\text{NO}_3)_2$, KNO_3 , LiNO_3 , $\text{Mg}(\text{NO}_3)_2 \cdot 6\text{H}_2\text{O}$, $\text{Mn}(\text{NO}_3)_2$, NaNO_3 , $\text{Ni}(\text{NO}_3)_2 \cdot 6\text{H}_2\text{O}$, $\text{Zn}(\text{NO}_3)_2 \cdot 6\text{H}_2\text{O}$, respectively, and were dissolved in distilled water. Thin-layer chromatography (TLC) was conducted on silica gel 60F₂₅₄ plate. All reactions were monitored by TLC with UV indicator (Shanghai Jiapeng Technology Co. Ltd., China). HEPES (4-(2-hydroxyethyl)-1-piperazineethanesulfonic acid) buffer solutions (pH 7.2) were prepared using 20 mM HEPES, and defined amount of aqueous sodium hydroxide under adjustment by a pH meter. Britton–Robinson (B–R) buffers were mixed by 40 mM acetic acid, boric acid, and phosphoric acid. Dilute hydrochloric acid or sodium hydroxide was used for tuning pH values. ^1H NMR and ^{13}C NMR spectra (at 400 MHz and 100 MHz, respectively) were recorded on a Bruker Avance 400 FT

spectrometer, using CDCl_3 as solvent and TMS as internal standard. CDCl_3 was used as delivered from Adamas Co., Ltd. (Shanghai, China). Chemical shifts were reported in parts per million. HRMS spectra were recorded on a Q-TOF6510 spectrophotometer (Agilent). UV-vis spectra were recorded on a UV-2550 (Hitachi). Fluorescent measurements were recorded on a F-4500 FL Spectrophotometer (Hitachi). The pH measurements were performed on a PHS-3C digital pH-meter (Mettler Toledo, America). Images of HeLa cells were captured with a laser confocal microscope (Carl Zeiss LSM-700, Germany).

Synthesis of probe L

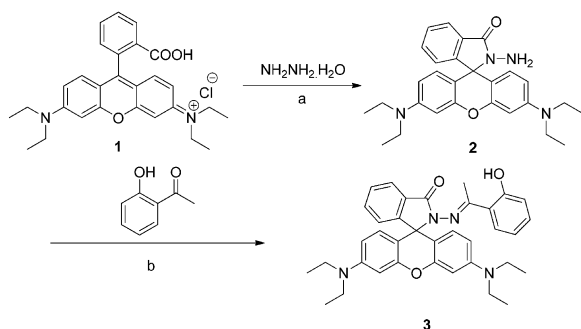
The synthetic route of **L** is shown in Scheme 1. Rhodamine hydrazide **2** was obtained by the reaction of $\text{NH}_2\text{NH}_2 \cdot \text{H}_2\text{O}$ (0.050 mmol, 2.0 equiv.) with rhodamine-B **1** (0.025 mmol, 1.0 equiv.) in refluxed ethanol (50 mL) without further purification.¹⁹ Then the solution of rhodamine hydrazide **2** (0.025 mmol, 1.0 equiv.) and *o*-hydroxy acetophenone (0.100 mmol, 4.0 equiv.) in ethanol (20 mL) was heated to reflux for 10 h and monitored by TLC. After the completion of the reaction, the mixture was evaporated to dryness and to the residue was added water. The extraction by ethyl acetate (20 mL) from the water for three times and further recrystallization from ethyl acetate afforded the target probe. The probe **L** was obtained as white solid in 91.7% yield. m.p. 170–172 °C ^1H NMR (400 MHz, CDCl_3) δ : 1.15 (t, $J = 7.0$ Hz, 12H), 2.31 (s, 3H), 3.32 (q, $J = 7.0$ Hz, 8H), 6.30 (dd, $J = 8.9, 2.6$ Hz, 2H), 6.40 (d, $J = 2.6$ Hz, 2H), 6.57 (d, $J = 8.9$ Hz, 2H), 6.71–6.85 (m, 2H), 7.12–7.23 (m, 2H), 7.43–7.57 (m, 3H), 7.87–8.01 (m, 1H), 11.76 (s, 1H) ppm; ^{13}C NMR (100 MHz, CDCl_3) δ : 12.6, 17.7, 44.4, 67.1, 98.2, 105.3, 108.1, 117.9, 118.1, 119.2, 123.2, 124.2, 128.2, 128.3, 129.0, 130.1, 132.1, 132.8, 148.9, 151.7, 153.5, 160.2, 161.6, 173.5 ppm. HRESIMS m/z : calcd for $[\text{M} + \text{H}]^+ \text{C}_{36}\text{H}_{39}\text{N}_4\text{O}_3$: 575.3017, found: 575.3009.

Preparation of probe solution

The mixture of 1 mL probe **L** at 100 μM in EtOH, 2.6 mL EtOH and 0.4 mL HEPES gave 4.0 mL probe **L** at 25 μM for UV, fluorescence detection and cell imaging. For the detection of the pH effect on the probe, 1.0 mL 100 μM probe **L**, 0.8 mL EtOH, 0.2 mL HEPES and 2.0 mL B–R buffers at the corresponding pH were used to give the 4.0 mL probe solution.

HeLa cell culture and imaging

HeLa cells were cultured in Dulbecco's modified Eagle's medium (DMEM, Gibco) containing 10% calf bovine serum 50 (HyClone) at 37 °C in humidified air and 5% CO_2 . The cells were subcultured at 90% confluence with 0.25% trypsin (w/v) every 2–3 days. For fluorescence, the cells were seeded into 10 mL centrifuge tube, and the experiments to assay Al^{3+} uptake were undertaken in the tube supplemented with 50 μM , 100 μM or 150 μM of $\text{Al}(\text{NO}_3)_3$ for 1 h respectively. Then the cells were washed with PBS (Phosphate Buffer Saline) twice and incubated with 10 μM probe **L** for 3 h. After being washed by PBS twice, the HeLa cells were imaged under a laser confocal microscope.



Scheme 1 Synthesis of the probe **L** reagents and conditions: (a) ethanol, reflux, 24 h; (b) ethanol, reflux, 10 h.

Cytotoxicity assay

The cells were seeded in 96-well plates at an initial density of 6000 cells per well, with 0.1 mL medium per well. After incubation for 12 h, HeLa cells were treated with probe **L** (5, 10, 15 and 15 μM). The MTT assay was used to detect cell cytotoxicity. Briefly, cells were incubated for 4 h with the tetrazolium salt (3-(4,5-dimethylthiazol-2-yl)-2,5-diphenyl tetrazolium enbromide) with a final concentration of 500 $\mu\text{g mL}^{-1}$, and metabolically active cells reduced the dye to purple formazan. Dark blue crystals were dissolved with 150 μL DMSO. The absorbance of the DMSO solution was measured with a BIO RAD microplate reader (model360, Hercules, California USA) at 490 nm.

Results and discussion

Synthesis and structural characterization

The reaction of $\text{NH}_2\text{NH}_2 \cdot \text{H}_2\text{O}$ and rhodamine-B **1** in ethanol afforded rhodamine hydrazide **2**, which then underwent a condensation with *o*-hydroxyacetophenone in refluxing ethanol, giving the target molecule **3**, *i.e.* **L** (Scheme 1). Furthermore, the structure of the target molecule **L** was determined by ^1H NMR, ^{13}C NMR and HRMS.

Colorimetric recognition

The absorption response of **L** (25 μM) toward a variety of metal ions was initially detected in EtOH/HEPES (9 : 1, v/v, pH 7.2) solution in the presence of 20 equiv. of different metal ions and the results were presented in Fig. S1†. The probe **L** was colorless and exhibited no scarcely absorption at 450–650 nm in this buffer solution, in agreement with the previous report,³⁴ suggesting that the **L** existed as a spirocycle-closed form. Whereas upon adding 20 equiv. various metal ions, a new absorption band centered at 560 nm was recognized among Cu^{2+} , Fe^{3+} , Ni^{2+} and Al^{3+} , which indicated that the probe **L** has the ability to sense these four metal ions by naked eyes.

Fluorescent recognition of Al^{3+}

Aiming at further exploring the possibility of **L** as an efficient probe, fluorescence spectra of **L** was examined on different kinds of metal ions. Among the four metal ions which could response in the colorimetric recognition, besides that the Fe^{3+} and **L** manifested a faint emission, only the purple solution of **L** and Al^{3+} exhibited a very strong emission, however, other metal ions did not induce any significant fluorescence enhancement (Fig. 1), which suggested that the **L** might be an ideal probe for sensing Al^{3+} by fluorescence spectra. The fluorescence reached peak in the solution EtOH/HEPES (9 : 1, v/v, pH 7.2) (Fig. S2†). Then in the optimized solution, competition experiments were carried out by detecting the variation in fluorescence intensity at 578 nm upon 20 equiv. Al^{3+} ion to a solution of **L** and different metal ions (20 equiv.) (Fig. 2). It could be noticed that besides Cu^{2+} none of these metal ions exerted any interference on the fluorescence intensity, suggesting that the probe **L** possessed the ability to sense Al^{3+} with high selectivity and efficiency. Besides, the solution of the probe **L** and Al^{3+} had a quantum yield of 0.29 in EtOH/HEPES (9 : 1, v/v, pH 7.2) at an excitation

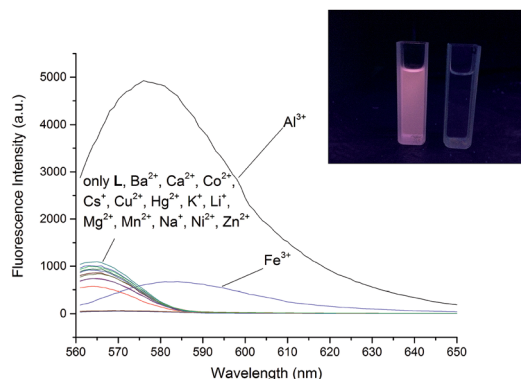


Fig. 1 Fluorescence spectra of 25 μM **L** in buffered EtOH/HEPES (9 : 1, v/v, pH 7.2) solution with 20 equiv. of metal ions. The inset showed the fluorescence color of **L** with Al^{3+} (left) and only **L** (right) (excitation wavelength: λ_{ex} = 560 nm; slit width, 10 nm; λ_{em} = 578 nm, slit width, 5 nm).

wavelength of 560 nm, based on optically matching solutions of rhodamine B standard (Φ = 0.69 in ethanol).

Then the titration experiment was performed in buffered solution by adding Al^{3+} (0–50 equiv.) into 25 μM of probe **L** and the results were presented in Fig. 3. The fluorescence emission intensity increased gradually upon the addition of Al^{3+} and enhanced dramatically about 43-fold when 10 equiv. Al^{3+} was added. When more Al^{3+} was titrated, instead of increasing significantly, the fluorescence intensity presented as a faint variation. The detection limit, based on the definition by IUPAC ($D_L = 3\text{Sb}/Cm$; Sb: the range of detection result; C : coefficient of range; m : the slope of the fitted curve), acquired from the linear of response range covering the Al^{3+} concentration from 0 to $2.5 \times 10^{-5} \text{ M}$, was calculated to be $1.63 \times 10^{-7} \text{ M}$ (Fig. S3†).

Besides, on the basement of linear fitting of Benesi–Hildebrand plot of Al^{3+} (1–9 equiv.) (Fig. S4†) with correlation coefficient over 0.99, the binding mode was recognized as 2 : 1 binding stoichiometry of **L** and Al^{3+} , which was further confirmed by Job's plot (Fig. S5†). In addition, the binding constant K_s was also calculated to be $1.17 \times 10^6 \text{ M}^{-1}$.

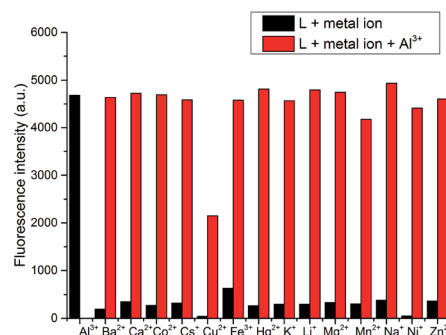


Fig. 2 Fluorescence intensity changes of 25 μM **L** to 20 equiv. of different metal ions in EtOH/HEPES (9 : 1, v/v, pH 7.2) buffered solution (black bars), and the fluorescence intensity changes when 20 equiv. Al^{3+} ion was added to the mixture of **L** (25 μM) and 20 equiv. different metal ions in the buffered solution, respectively (red bars). λ_{ex} = 560 nm, λ_{em} = 578 nm.

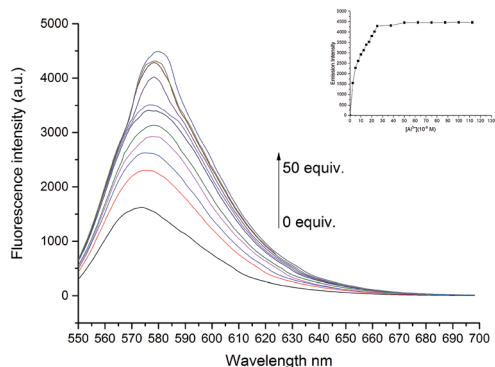


Fig. 3 Fluorescence response of **L** (25 μM) in buffered EtOH/HEPES (9 : 1, v/v, pH 7.2) solution on the addition of Al^{3+} (0–10 equiv.). λ_{ex} = 560 nm, λ_{em} = 578 nm.

We then investigated on the specific binding structure of **L** and Al^{3+} with the assistance of ^1H NMR and ^{13}C NMR spectroscopy. In detail, interestingly, upon the addition of Al^{3+} , the sharp peak at 11.73 ppm (for the OH proton) was reduced and a new peak at 9.25 ppm could be found in ^1H NMR spectra which might attribute to the proton of the OH in the newly formed complex and in the ^{13}C NMR spectra the peak at 44.14 ppm (for the carbon atom of CH_3 near OH) converted to two peaks in the ^{13}C NMR (Fig. 4). Based on the previous articles^{38,39} and the binding stoichiometry along with the alternations in the ^1H NMR and ^{13}C NMR spectroscopy, the proposed reaction mechanism of **L** and Al^{3+} was predicted in Fig. 5.

We then explored the effect of time and pH value on the probe **L**. To our delight, the curves (Fig. 6) of response time revealed that **L** could form complex with 20 equiv. Al^{3+} completely within 1 min, after which the fluorescence intensity remained constant in the following 30 min, indicating that the complex thus formed possessed perfect stability. In terms of pH effect, the fluorescence intensity did not change significantly as pH converted from 4.88 to 8.53 (Fig. S6[†]), whereas a sudden variation was observed when the pH was over 9.

Furthermore, to examine the reversibility of the binding of **L** to Al^{3+} , we used EDTA, a well-known metal ion chelator in buffered EtOH/HEPES solutions. The fluorescence intensity of **L**– Al^{3+} (25 μM) at 578 nm was almost totally quenched by the

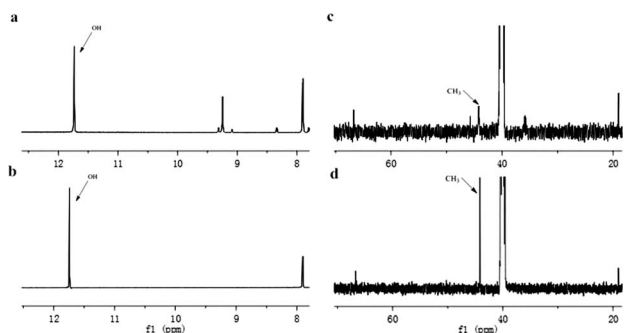


Fig. 4 Partial ^1H NMR spectra of (a) probe **L**, (b) **L** in the presence of Al^{3+} . Partial ^{13}C NMR spectra of (c) probe **L**, (d) **L** in the presence of Al^{3+} .

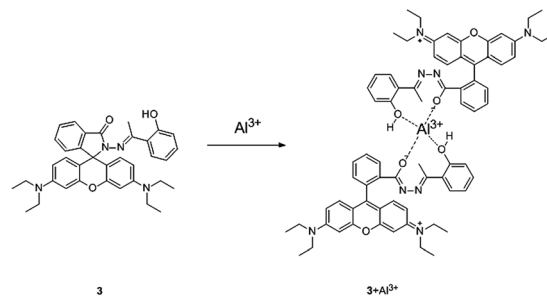


Fig. 5 The plausible reaction mechanism of **L** and Al^{3+} .

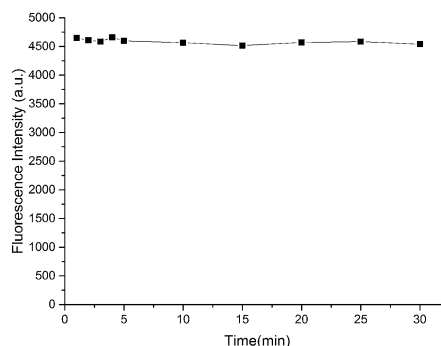


Fig. 6 Time dependence of fluorescence response of **L** (25 μM) in buffered EtOH/HEPES (9 : 1, v/v, pH 7.2) solution with 20 equiv. Al^{3+} . λ_{ex} = 560 nm, λ_{em} = 578 nm.

addition of 1.0 equiv. of EDTA (Fig. 7). Then the fluorescence intensity recovered with the addition of Al^{3+} to the mixture of **L**– Al^{3+} –EDTA (25 μM). It could be inferred that the selective binding of **L** and Al^{3+} was easily reversible and **L** would perform as a recycle probe in practical utilization.

Fluorescent imaging of intercellular Al^{3+}

To investigate the potential application of probe **L** in living cells, we performed the intercellular Al^{3+} imaging of HeLa cells by a laser confocal microscope (Fig. 8). After incubation with 10 μM of **L** for 1 h at 37 $^{\circ}\text{C}$, no obvious fluorescence emission was intracellular, which was in agreement with the property of the **L** discovered in our previous study. However, when different concentrations of Al^{3+} was added to the growth medium to incubate HeLa cells for 1 h, the same treatment with **L** would generate significant intracellular fluorescence. As with the increasing Al^{3+} concentration in incubated cells, the intracellular fluorescence enhanced dramatically, indicating that dose-dependent response of **L** to Al^{3+} could be applied in live cells as well. Furthermore, contrary to the other Al^{3+} probes with poor water solubility which were impermeable to the physiological conditions, **L** could permeate into the HeLa cells within 1 h.

MTT toxicity assay

The toxicity of probe **L** in HeLa cells was assayed by MTT method by the incubation of the cells with **L** at different concentrations for 48 h (Fig. 9). Even with the high

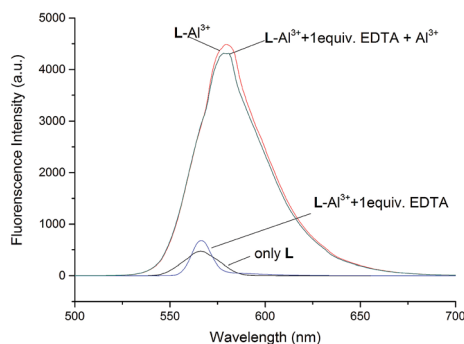


Fig. 7 Reversibility of L-Al³⁺ binding (25 μ M) in buffered EtOH/HEPES (9 : 1, v/v, pH 7.2) solution. λ_{ex} = 560 nm, λ_{em} = 578 nm.

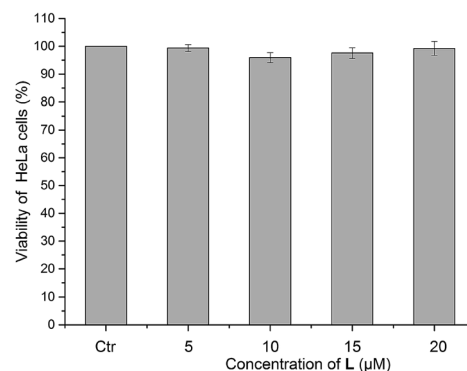


Fig. 9 The viability of HeLa cells after incubation with different concentrations of probe L for 24 h (the viability was tested by MTT assay with $n = 5$ replicates).

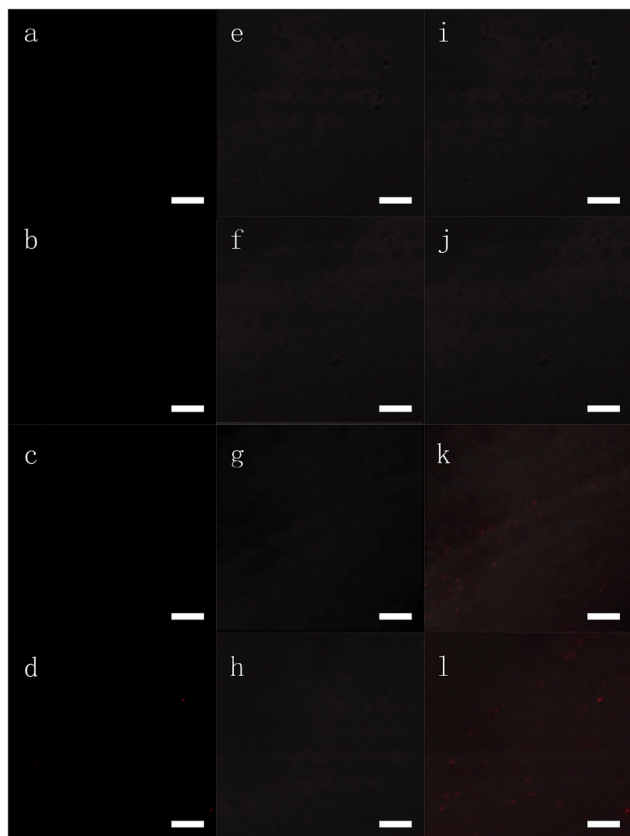


Fig. 8 (a) HeLa cells incubated with 10 μ M probe for 1 h at 37 $^{\circ}$ C (b) HeLa cells incubated with 25 μ M Al³⁺ added to the growth medium for 1 h at 37 $^{\circ}$ C and then incubated with 10 μ M probe for 1 h. (c) HeLa cells incubated with 50 μ M Al³⁺ added to the growth medium for 1 h at 37 $^{\circ}$ C and then incubated with 10 μ M probe for 1 h at 37 $^{\circ}$ C. (d) HeLa cells incubated with 75 μ M Al³⁺ added to the growth medium for 1 h at 37 $^{\circ}$ C and then incubated with 10 μ M probe for 1 h at 37 $^{\circ}$ C. (e) Bright-field view of panel (a). (f) Bright-field view of panel (b). (g) Bright-field view of panel (c). (h) Bright-field view of panel (d). (i) Overlay image of (a) and (e). (j) Overlay image of (b) and (f). (k) Overlay image of (c) and (g). (l) Overlay image of (d) and (h). Scale bars: all images = 10 μ m.

concentration at 20 μ M, 2-fold higher than the general concentration used in imaging experiment, the viability of HeLa cells remained at $99.2 \pm 2.5\%$. Therefore, probe L was non-toxic

to cells and thus safely to be applied in cell marking and clinical use in physiological conditions.

Conclusions

In summary, the first rhodamine-based probe L for fluorescent recognition of Al³⁺ in living cells was designed and synthesized. The fluorescence intensity of the probe enhanced 43-fold and the color of L in the buffer solution changed from colorless to purple with the addition of Al³⁺. Probe L could serve as a fluorescent indicator for Al³⁺ without any inference from other metal ions, at a wide pH ranging from 4.9 to 8.5. Besides, the detection limit of L was $1.63 \times 10^{-7} \text{ M}^{-1}$ and L possessed perfect stability and excellent reversibility. Finally, probe L has been successfully applied to the imaging for sensing Al³⁺ in HeLa cells in fluorescence protocol and was proved to be non-toxic to living cells by MTT assay.

Acknowledgements

We would like to thank the National Natural Science Foundation of China (21002081) and the Fundamental Research Funds for the Central Universities, P.R. China (XDJK2012B012) for financial support.

Notes and references

- 1 H. N. Kim, Z. Guo, W. Zhu, J. Yoon and H. Tian, *Chem. Soc. Rev.*, 2011, **40**, 79–93.
- 2 H. N. Kim, W. X. Ren, J. S. Kim and J. Yoon, *Chem. Soc. Rev.*, 2012, **41**, 3210–3244.
- 3 D. T. Quang and J. S. Kim, *Chem. Rev.*, 2010, **110**, 6280–6301.
- 4 J. S. Kim and D. T. Quang, *Chem. Rev.*, 2007, **107**, 3780–3799.
- 5 V. Luxami and S. Kumar, *RSC Adv.*, 2012, **2**, 8734–8740.
- 6 Z. Xu, N. J. Singh, J. Lim, J. Pan, H. N. Kim, S. Park, K. S. Kim and J. Yoon, *J. Am. Chem. Soc.*, 2009, **131**, 15528–15533.
- 7 J. H. Jung, D. S. Cheon, F. Liu, K. B. Lee and T. S. Seo, *Angew. Chem., Int. Ed.*, 2010, **49**, 5708–5711.
- 8 D. Knapton, M. Burnworth, S. J. Rowan and C. Weder, *Angew. Chem., Int. Ed.*, 2006, **45**, 5825–5829.

- 9 R. C. Stringer, S. Gangopadhyay and S. A. Grant, *Anal. Chem.*, 2010, **82**, 4015–4019.
- 10 T. Naddo, X. Yang, J. S. Moore and L. Zang, *Sens. Actuators, B*, 2008, **134**, 287–291.
- 11 B. Sun, W. Xie, G. Yi, D. Chen, Y. Zhou and J. Cheng, *J. Immunol. Methods*, 2001, **249**, 85–89.
- 12 M. de la Guardia, A. R. Mauri and C. Mongay, *J. Anal. At. Spectrom.*, 1988, **3**, 1035–1038.
- 13 W. J. McShane, R. S. Pappas, V. Wilson-McElprang and D. Paschal, *Spectrochim. Acta, Part B*, 2008, **63**, 638–644.
- 14 R. B. Martin, *Acc. Chem. Res.*, 1994, **27**, 204–210.
- 15 E. Delhaize and P. R. Ryan, *Plant Physiol.*, 1995, **107**, 315–321.
- 16 M. Venturini-Soriano and G. Berthon, *J. Inorg. Biochem.*, 2001, **85**, 143–154.
- 17 R. J. P. Williams, *Coord. Chem. Rev.*, 2002, **228**, 93–96.
- 18 S. Mazzaferro, I. Perruzza, S. Costantini, M. Pasquali, L. Onorato, D. Sardella, R. Giordano, L. Ciaralli, P. Ballanti, E. Bonucci, G. A. Cinotti and G. Coen, *Nephrol., Dial., Transplant.*, 1997, **12**, 2679–2682.
- 19 P. F. Good, C. W. Olanow and D. P. Perl, *Brain Res.*, 1992, **593**, 343–346.
- 20 J. Barceló and C. Poschenrieder, *Environ. Exp. Bot.*, 2002, **48**, 75–92.
- 21 K. Soroka, R. S. Vithanage, D. A. Phillips, B. Walker and P. K. Dasgupta, *Anal. Chem.*, 1987, **59**, 629–636.
- 22 Y. Zhao, Z. Lin, H. Liao, C. Duan and Q. Meng, *Inorg. Chem. Commun.*, 2006, **9**, 966–968.
- 23 C. Gou, S.-H. Qin, H.-Q. Wu, Y. Wang, J. Luo and X.-Y. Liu, *Inorg. Chem. Commun.*, 2011, **14**, 1622–1625.
- 24 S. M. Ng and R. Narayanaswamy, *Anal. Bioanal. Chem.*, 2006, **386**, 1235–1244.
- 25 D. Maity and T. Govindaraju, *Chem. Commun.*, 2010, **46**, 4499–4501.
- 26 S. Sinha, R. R. Koner, S. Kumar, J. Mathew, P. V. Monisha, I. Kazi and S. Ghosh, *RSC Adv.*, 2013, **3**, 345–351.
- 27 J. Y. Kwon, Y. J. Jang, Y. J. Lee, K. M. Kim, M. S. Seo, W. Nam and J. Yoon, *J. Am. Chem. Soc.*, 2005, **127**, 10107–10111.
- 28 Y.-K. Yang, K.-J. Yook and J. Tae, *J. Am. Chem. Soc.*, 2005, **127**, 16760–16761.
- 29 V. Dujols, F. Ford and A. W. Czarnik, *J. Am. Chem. Soc.*, 1997, **119**, 7386–7387.
- 30 M. Vendrell, D. Zhai, J. C. Er and Y. T. Chang, *Chem. Rev.*, 2012, **112**, 4391–4420.
- 31 H. N. Kim, M. H. Lee, H. J. Kim, J. S. Kim and J. Yoon, *Chem. Soc. Rev.*, 2008, **37**, 1465–1472.
- 32 A. Chatterjee, M. Santra, N. Won, S. Kim, J. K. Kim, S. B. Kim and K. H. Ahn, *J. Am. Chem. Soc.*, 2009, **131**, 2040–2041.
- 33 Y. Xiang, A. Tong, P. Jin and Y. Ju, *Org. Lett.*, 2006, **8**, 2863–2866.
- 34 W. Y. Liu, S. L. Shen, H. Y. Li, J. Y. Miao and B. X. Zhao, *Anal. Chim. Acta*, 2013, **791**, 65–71.
- 35 F. Ge, H. Ye, J.-Z. Luo, S. Wang, Y.-J. Sun, B.-X. Zhao and J.-Y. Miao, *Sens. Actuators, B*, 2013, **181**, 215–220.
- 36 H. Ye, F. Ge, X.-C. Chen, Y. Li, H. Zhang, B.-X. Zhao and J.-Y. Miao, *Sens. Actuators, B*, 2013, **182**, 273–279.
- 37 H. Yang, Z. Zhou, K. Huang, M. Yu, F. Li, T. Yi and C. Huang, *Org. Lett.*, 2007, **9**, 4729–4732.
- 38 K. Huang, H. Yang, Z. Zhou, M. Yu, F. Li, X. Gao, T. Yi and C. Huang, *Org. Lett.*, 2008, **10**, 2557–2560.
- 39 M. Li, H.-S. Lv, J.-Z. Luo, J.-Y. Miao and B.-X. Zhao, *Sens. Actuators, B*, 2013, **188**, 1235–1240.
- 40 W.-Y. Liu, H.-Y. Li, H.-S. Lv, B.-X. Zhao and J.-Y. Miao, *Spectrochim. Acta, Part A*, 2012, **95**, 658–663.
- 41 W.-Y. Liu, H.-Y. Li, B.-X. Zhao and J.-Y. Miao, *Org. Biomol. Chem.*, 2011, **9**, 4802–4805.